



# Technical report: Modelling the August 2021 COVID-19 outbreak in New Zealand

Michael Plank, Shaun Hendy, Rachelle Binny, Oliver Maclaren

18 October 2021

## Executive Summary

- We use a branching process model to simulate the Auckland August 2021 outbreak through to early January 2022, including the effects of increasing vaccine coverage by age group and time.
- Based on vaccination data and bookings for the Auckland metro region, we estimate that vaccination reduces the model reproduction number by approximately 67% relative to an unvaccinated population by early January 2022.
- We assume that Alert Level 3 controls are held in place and that the effect of these controls does not diminish over time. Effective contact tracing capacity is set at 1,000 active cases.
- In low-transmission scenarios, vaccination in tandem with sustained alert level restrictions is sufficient to bring  $R_{eff} < 1$  in November. These scenarios generally lead to case numbers that are likely to be manageable within existing health system capacity.
- In high-transmission scenarios, vaccination and current alert level restrictions are not sufficient to bring  $R_{eff} < 1$  during 2021. These scenarios generally lead to case numbers that would place extreme demands on health system capacity.
- In the high-transmission scenario, an effective two-week Alert Level 4 ‘circuit breaker’ in early November followed by a return to Alert Level 3 can significantly reduce demand on the health care system through to the beginning of 2022.

## Introduction

This report covers modelling carried out from late September through to mid-October 2021 of the Auckland August 2021 outbreak of COVID-19. We simulate the outbreak through to the beginning of 2022, considering the effects of increasing vaccine coverage by age group and time, as well as targeted and population-wide control measures. We use vaccine booking data from the Auckland metro region up to 13 October 2021 to project that approximately 87% of the eligible population (over 12 years old) will have received at least one dose by early November and be fully vaccinated by the end of December 2021. Note that our reported coverage estimates are based on the proportion of the estimated residential population, rather than the health service utilisation population used by the Ministry of Health, so are lower than official figures suggest (see Methods). In the simulations considered here, we assume that Alert Level 3 controls are held in place until the end of the simulation. If the outbreak is well controlled and health care capacity is not threatened, it may be possible to ease restrictions earlier than this.

Our model analysis comes in two parts. Firstly, we estimate a time-varying effective reproduction number  $R_{eff}$  by fitting the branching process model and case data between 17 August 2021 and 15 October 2021. This  $R_{eff}$  represents the combined, time-varying



effectiveness of alert level restrictions and increasing vaccine coverage. The effectiveness of alert level restrictions is allowed to vary between 17 August and 6 October, but is assumed to be constant from 6 October as there is not yet sufficient data to robustly estimate any change in transmission rate subsequent to this date.

Secondly, we consider a range of future scenarios based on running the model forward until early January 2022, assuming a constant alert level effectiveness from 6 October 2021, along with vaccine coverage that continues to increase as estimated from vaccination booking data. The values for the alert level effectiveness considered in these scenarios approximately span the estimated range for the period since 6 October. Hence these scenarios represent plausible outcomes under current alert level restrictions, depending on whether transmission rates are towards the lower or the upper end of current estimates.

## Methods

We model transmission of SARS-CoV-2 using a stochastic age-structured branching process model (1). Infected individuals are categorised as either clinical or subclinical, with the clinical fraction  $p_{clin}$  increasing with age (see Table 1). Subclinical individuals are assumed to be  $\tau = 50\%$  as infectious as clinical individuals (2-4). Clinical individuals are assigned a symptom onset time which is gamma distributed from exposure time with mean 5.5 days and s.d. 3.3 days (5). In the absence of interventions, we assume generation times are drawn from a Weibull distribution with mean 5.0 days and s.d. 1.9 days (6). There is at present conflicting evidence in the literature as to whether the Delta variant of SARS-CoV-2 has a shorter mean generation time or mean incubation period than older variants (7-11). Generation times in particular are difficult to empirically measure because this requires the infection times of both cases in a transmission pair. If infection times are unavailable but symptom onset dates are known, the serial interval can be used as a proxy for generation time. However, serial interval measurements contain more noise as they depend on both individuals' incubation periods. In addition, for both generation times and serial intervals, realised values are affected by control interventions such as test, trace and isolate measures.

### Test-trace-isolate-quarantine system model

We assume that the probability of case detection for all infected individuals (clinical and subclinical) after 17 August is  $p_{test} = 0.45$ , and detection occurs with an exponentially distributed delay from onset (or pseudo-onset for subclinical individuals) with mean 4 days. Although using an exponential distribution is a simplifying assumption, the coefficient of variation of the exponential distribution ( $CV = 1$ ) is similar to the coefficient of variation of observed data from the August 2021 outbreak on the time from symptom onset to reporting for cases designated as “sought healthcare” in EpiSurv ( $CV = 1.025$ ). The shape of the distribution is also approximately consistent with onset to reporting times from the August 2020 outbreak. Furthermore, we note that, for a given overall effect of TTIQ on  $R_{eff}$  (see next paragraph), model results are not highly sensitive to the shape of the assumed onset to detection distribution.

We assume that a proportion  $p_{trace} = 0.7$  of secondary infections of a confirmed case are identified via contact tracing and quarantined with a mean of 3 days from confirmation of the index case. In reality, some contacts are scheduled for testing on day 5 and day 12 after exposure and management differs for close and casual contacts; however, we do not attempt



to model the contact tracing process at this level of detail. We use quarantine to refer to pre-symptomatic or asymptomatic individuals identified via contact tracing who have not yet returned a positive test result, and isolation to refer to individuals who have either developed symptoms or tested positive. We assume quarantine reduces transmission by 50% and more stringent isolation prevents all further transmission. The estimated overall reduction in  $R_{eff}$  from these measures is approximately 20%.

## Vaccine effectiveness and coverage

Vaccine effectiveness is characterised by three parameters: effectiveness against infection ( $e_I$ ), effectiveness against transmission in breakthrough infections ( $e_T$ ), and effectiveness against severe disease or death in breakthrough infections ( $e_D$ ) for the Pfizer/BioNTech mRNA vaccine – see Supplementary Table S1 (12, 13). The number of people in each age group who have received one or two doses of the vaccine is time-varying based on vaccinations already administered, as well as Ministry of Health data on future bookings, using data for the Auckland metro region current at 13 October 2021 (Figure 1). In addition, we assume that everyone who has received or has booked an appointment for their first dose will eventually receive their second dose. For those who have had their first dose but do not have an appointment booked for their second dose, the time of the second dose is assumed to be uniformly distributed in the 12 week period following 13 October 2021. Population denominators for each age band are taken to be the estimated resident population (ERP) according to StatsNZ. Under these assumptions, approximately 87% of the eligible population (over 12 years old) will have received at least one dose of the vaccine by mid November and will be fully vaccinated by early January 2022. Note that model vaccine coverage is lower than official Ministry of Health statistics because the latter use the health service utilisation (HSU) population, which is smaller than the ERP, as denominators. To model the delay in the immune response to vaccination, all vaccine doses are assumed to take effect 14 days after being administered.

## Age-structured transmission model

Transmission between age groups is described by a next generation matrix, whose  $(i,j)$  element is defined to be the expected number of secondary infections in age group  $i$  caused by an infected individual in age group  $j$  in the absence of control measures and given a fully susceptible population:

$$NGM_{ij} = U(p_{clin,j} + \tau(1 - p_{clin,j}))u_i M_{j,i}$$

where  $u_i$  is the relative susceptibility to infection of age group  $i$ ,  $M$  is a contact matrix describing mixing rates between and within age groups (14),  $U$  is a constant representing the intrinsic transmissibility of the virus. The basic reproduction number  $R_0$  is equal to the dominant eigenvalue of the next generation matrix, denoted  $\rho(NGM)$ . The value of  $U$  is chosen so that  $\rho(NGM)$  is equal to the assumed value of  $R_0 = 6$ .

The number of people in age group  $j$  infected by clinical individual  $l$  between time  $t$  and  $t + \delta t$  is a Poisson distributed random variable with mean

$$\lambda_{l,j}(t) = Y_l C(t) V_l(t) F_l(t) \left( \int_t^{t+\delta t} w(\tau - t_{inf,l}) d\tau \right) NGM_{j,a_l}^{clin} s_j(t)$$

where:

- $Y_l$  is a gamma distributed random variable with mean 1 and variance  $1/k$  representing individual heterogeneity in transmission. We set  $k = 0.5$  which represents a moderate



level of over-dispersion and is consistent with estimates for SARS-CoV-2 transmission patterns (15, 16).

- $C(t)$  is a time-varying control parameter that is fitted to data (see below).
- $V_l(t)$  represents the effect of vaccination on the transmission rate of individual  $l$ , and is equal to 1,  $1 - e_{T1}$ , or  $1 - e_{T2}$  if individual  $l$  is unvaccinated, has had one dose, or has had two doses respectively at time  $t$ .
- $F_l(t)$  represents the effect of quarantine or isolation on the transmission rate of individual  $l$  at time  $t$ , and is equal to 1 if individual  $l$  is not in quarantine/isolation at time  $t$ , equal to  $c_{quar} = 0.5$  if individual  $l$  is in quarantine, and equal to  $c_{isol} = 0$  if individual  $l$  is in isolation.
- $w(\tau)$  is the probability density function of the assumed generation time distribution and  $t_{inf,l}$  is the time individual  $l$  was infected.
- $NGM^{clin}$  is the next generation matrix for clinical individuals and  $a_l$  is the age group of individual  $l$ .
- $s_j(t)$  is the fraction of age group  $j$  that is susceptible at time  $t$ , defined by

$$s_j(t) = 1 - e_{I1}c_{j1}(t) - e_{I2}c_{j2}(t) - \frac{N_j(t)}{N_{j,tot}}$$

where  $c_{jd}(t)$  is the fraction of age group  $j$  that has received  $d$  effective doses of the vaccine at time  $t$ ,  $N_j(t)$  is the cumulative number of infections in age group  $j$  at time  $t$  and  $N_{j,tot}$  is the total size of age group  $j$ .

The expression for  $\lambda_{l,j}(t)$  above is multiplied by  $\tau$  if individual  $l$  is subclinical. Note that the factor  $Y_l$  means that, in the absence of control measures, the total number of people infected by a randomly selected individual has a negative binomial distribution with mean  $R_0$  and variance  $R_0(1 + R_0/k)$  (17).

The vaccination status of new infections in age group  $j$  at time  $t$  is assigned to be 0, 1 or 2 doses with respective probabilities

$$\begin{aligned} q_{j0}(t) &= \frac{1 - c_{j1}(t) - c_{j2}(t)}{1 - e_{I1}c_{j1}(t) - e_{I2}c_{j2}(t)} \\ q_{j1}(t) &= \frac{(1 - e_{I1})c_{j1}(t)}{1 - e_{I1}c_{j1}(t) - e_{I2}c_{j2}(t)} \\ q_{j2}(t) &= \frac{(1 - e_{I2})c_{j2}(t)}{1 - e_{I1}c_{j1}(t) - e_{I2}c_{j2}(t)} \end{aligned}$$

This models the effect of the vaccine as completely immunising a randomly selected fraction  $e_{Id}$  of individuals with  $d$  doses and leaving the remaining fraction  $1 - e_{Id}$  completely susceptible. This is known as an all-or-nothing vaccine model and is a simplification of the effect of vaccination on susceptibility to infection (18). An alternative model formulation is a leaky vaccine model, where all vaccinated individuals have their probability of infection reduced by  $e_I$ . Reality is likely to be somewhere between these idealised models (i.e. there is some individual heterogeneity in the level of protection provided by the vaccine but not as extreme as all-or-nothing). However, the all-or-nothing and the leaky vaccine model behave similarly when the proportion of the population with immunity from prior infection is relatively small. Waning of immunity from either vaccination or from prior infection is ignored.

The expected number of secondary infections in age group  $i$  caused by an infected individual in age group  $j$  in the absence of any control measures other than vaccination is:

$$NGM_{ij}^p(t) = (1 - e_{T1}q_{j1}(t) - e_{T2}q_{j2}(t))(1 - e_{I1}c_{i1}(t) - e_{I2}c_{i2}(t))NGM_{ij}$$



Outbreaks are initialised by seeding 135 infections uniformly distributed between 10 August and 17 August. The number of seed infections was chosen based on previous calibration of the model to data on the number of new daily cases in the early stages of the outbreak.

## Hospitalisation and fatality model

We consider a simplified model for clinical pathways. More detailed models based on estimates of ICU admission risk and length of stay in ward, ICU and stepdown care could be overlaid onto simulation outputs for the number of infections based on international studies or as more data from the current outbreak becomes available. Clinical individuals in age group  $i$  with  $d$  doses of the vaccine are assumed to require hospitalisation with probability  $(1 - e_{Dd})p_{hosp,i}/p_{clin,i}$  where  $e_{Dd}$  is the vaccine effectiveness against severe disease in breakthrough infections after  $d$  doses, and  $p_{hosp,i}$  is the infection to hospitalisation ratio for unvaccinated people in age group  $i$  (see Table 1). The time between symptom onset and hospitalisation is assumed to be exponentially distributed with mean 5 days (this assumption affects the timing but not the number of hospital admissions). The length of hospital stay is assumed to be exponentially distributed with mean 8 days (19) (this assumption affects the number of hospital beds occupied at any one time but not the total number of hospital admissions). Hospitalised cases in age group  $i$  die with probability  $IFR_i/p_{hosp,i}$  where  $IFR_i$  is the infection fatality ratio for unvaccinated cases in age group  $i$  (see Table 1). For simplicity, the date of death is assumed to be the same as the date of hospital discharge. In reality, the average time from hospital admission to death is longer (this assumption means that deaths will be more lagged relative to cases in reality than in the model but does not affect the total number of deaths).

## Time-dependent transmission and parameter inference

For simplicity, we assume that vaccination, case isolation, and alert level restrictions act independently to provide multiplicative reductions in  $R_{eff}$ . It is possible that vaccination and alert level restrictions do not act independently if, for example, vaccination rates differ for those who work from home during alert level restrictions. Under the model assumptions described above, vaccination at the 17 August coverage level reduces transmission by around 13% (from  $R_0 = 6.0$  to  $R_v = 5.0$ ). After the outbreak is detected, the effects of case isolation and contact tracing reduce transmission by a further 20%. The effect of different alert level restrictions is unknown and likely changing over time. To capture this effect, we introduce a time-varying control factor  $C(t)$  which acts multiplicatively on transmission rate at time  $t$ . This approach assumes that alert level restrictions only change the contact matrix  $C$  by an overall multiplicative factor. This is not completely realistic as contact rates between different age groups are likely to respond differently, but is a necessary model assumption in the absence of specific data to parameterise a time-dependent contact matrix. We estimate the value of  $C(t)$  by fitting model output to data on new daily cases, using an approximate Bayesian computation (ABC) approach (see below). For simplicity, we model  $C(t)$  as a piecewise constant function:  $C(t) = \theta_k$  when  $t_{k-1} \leq t < t_k$ , with  $t_1$  corresponding to 18 August 2021 (the first day of alert level 4) and  $t_2, \dots, t_7$  increasing in 7-day increments (see Figure 2a). This formulation allows for weekly changes in the effect of contact rates on transmission at a population level.

We use a truncated Gaussian random field as the prior for  $\theta = [\theta_1, \theta_2, \dots, \theta_K]$ . We sample from the prior by generating random deviates from a multivariate normal distribution and then



accepting non-negative realisations. The multivariate normal distribution has mean  $\mu = [1, 0.5, \dots, 0.5]$ , and covariance matrix  $\Sigma = DCD$ , where  $D$  is a diagonal matrix of standard deviations with elements  $D_{kk} = [0.2, 0.5, \dots, 0.5]$  and  $C_{kl} = \exp(-(k-l)^2/2L^2)$  is the correlation matrix. This matrix has squared exponential form with correlation length  $L = 2$ , reflecting an *a priori* assumption that the control function (reduction in transmission) value in a given week is similar (but not identical) to its value in preceding weeks. The precise hyperparameter choices do not have a large impact on results, and together represent a relatively uninformative prior for the transmission rates during the period of alert level restrictions (see Supplementary Figure S1). The higher value for  $\mu_1$  and smaller value for  $D_{11}$  represent a narrower prior around  $C(t) = 1$  (i.e. no reduction in transmission) during the period before the outbreak was detected.

Given the above prior, a posterior distribution for the values of  $C(t)$  is obtained by conditioning on data on the number of new daily cases. We do this using an ABC method with sequential Monte Carlo (ABCSCMC). The algorithm proceeds as follows (20):

1. Set population indicator  $m = 1$ ,
2. If  $m = 1$ , sample a proposal value  $\theta^{prop}$  independently from the prior.  
Else sample  $\theta^*$  from the previous population  $\{\theta_{m-1}^{(n)}\}$  with weights  $w_{m-1}^{(n)}$  and perturb the particle to obtain  $\theta^{prop} \sim K_m(\theta| \theta^*)$ , where  $K_m$  is a Gaussian perturbation kernel with zero mean. The covariance matrix for the perturbation kernel is set to be  $0.5\Sigma$  if  $m = 1$  and to be a diagonal matrix with elements equal to  $2Var(\theta_{m-1}^{(n)})$  if  $m > 1$ . If  $\pi(\theta^{prop}) = 0$ , repeat step 2.
3. Generate one realisation of the branching process model with  $\theta = \theta^{prop}$ , record the time series  $x^{prop}$  of daily reported cases and calculate the distance function  $d(x^{prop}, x^{data})$ .
4. Repeats of steps 2-3 until: (i) at least  $N$  particles have been obtained with distance  $d(x^{prop}, x^{data}) \leq \varepsilon_m$ ; and (ii) at least  $N/\alpha_m$  proposal values have been simulated, guaranteeing an acceptance rate of at most  $\alpha_m$ .
5. Set the  $m^{th}$  population  $\{\theta_m^{(n)}\}, n = 1, \dots, N$  to be the  $N$  particles with the smallest values of  $d(x^{prop}, x^{data})$ .
6. Calculate the weight for particle  $\theta_m^{(n)}$ ,
$$w_m^{(n)} = \begin{cases} 1, & \text{if } m = 1 \\ \frac{\pi(\theta_m^{(n)})}{\sum_{j=1}^N w_{m-1}^{(j)} K_m(\theta_{m-1}^{(j)}, \theta_m^{(n)})} & \text{if } m > 1 \end{cases}$$
7. If  $m < M$ , set  $m = m + 1$  and go to step 2.

We define the distance function on time series of daily reported cases  $x = \{x_i\}$  to be the sum of squared errors on square-root transformed data:

$$d(x, y) = \sum_i (\sqrt{x_i} - \sqrt{y_i})^2$$

Using the sum of squared errors without the square-root transform leads to very similar results. We use a maximum acceptance rate of  $\alpha_m = 0.01$ , distance thresholds  $\varepsilon_1 = 240$ ,  $\varepsilon_{m+1} = 0.8\varepsilon_m$ , and simulate  $M = 3$  populations of  $N = 1000$  particles each. This combination of hyperparameters was found to give a reasonable combination of runtime and improvement in model fit for each population of particles. Typically, the first specified threshold  $\varepsilon_1$  is the binding constraint for the first population, but the maximum acceptance rate  $\alpha_m$  is the binding constraint for subsequent populations, with the realised distance value being substantially smaller than the specified threshold  $\varepsilon_m$ . Using a fourth population of particles ( $M = 4$ ) only



provided a small improvement in model fit. The final population of particles  $\{\theta_M^{(n)}\}$  is taken to be an approximation of the posterior distribution for  $\theta$ .

The data  $x_{data}$  is defined to be the number of new reported cases on each day between 17 August 2021 and a cut-off date of 15 October 2021, using the *Date reported* field in EpiSurv. This ignores spatial and demographic heterogeneity and possible regional differences in transmission, for example for the cases in the Waikato. It also ignores regional differences in vaccination rates: we use data on vaccinations for the Auckland metro region, since this is where the great majority of cases have been. In future, it would be possible to run the model using national vaccine coverage data if the outbreak becomes more geographically widespread.

Projected case numbers are based on independent model simulations with values of  $\theta$  drawn from the estimated posterior distribution. The time-varying value of  $R_{eff}(t)$  is a model output defined as

$$R_{eff}(t) = C(t)(1 - E)\rho(NGM^v(t))$$

where  $\rho(NGM^v)$  is the dominant eigenvalue of the next generation matrix with the vaccine coverage at time  $t$ , and  $E$  is the effectiveness of the test-trace-isolate-quarantine (TTIQ) system in the model in reducing transmission. The value of  $E$  is calculated by calculating the average reduction in transmission from the time each case is put into quarantine or isolation. For the assumed TTIQ parameters shown in Supplementary Table S1,  $E$  is approximately 0.2.

## Results and discussion

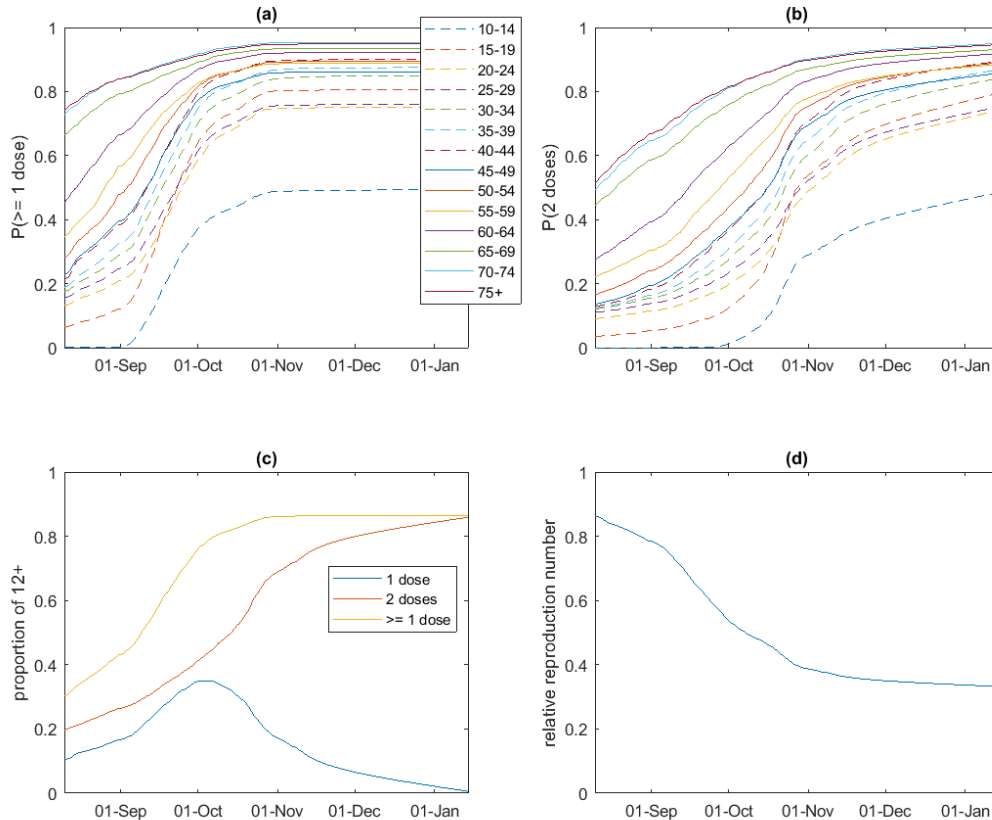
### Model calibration and estimating time-varying alert level effectiveness

Figure 1 shows the assumed vaccine coverage by age group and time and its modelled effect on the reproduction number. Vaccination reduces the model reproduction number by 67% relative to an unvaccinated population by early January 2022. Note that the vaccination bookings data does not capture people who get vaccinated without a prior appointment. If future vaccinations significantly outpace bookings, the reproduction number will decline more rapidly than shown in Fig. 1(d). Figure 2 shows the fitted control function  $C(t)$  and the time-varying reproduction number  $R_{eff}(t)$ , which depends on the value of the control function and the vaccine coverage at time  $t$ . A large reduction in transmission is evident following the move to alert level 4 on 18 August 2021. This was followed by an increase in transmission rates in weeks 4 and 5 of the alert level 4 period, consistent with the flattening out of case numbers around this time. The move from alert level 4 to alert level 3 on 22 September 2021 was associated with a further increase in transmission.

Figure 3 shows key model outputs from 1000 simulations with  $\theta$  drawn independently from the estimated posterior distribution, and assuming alert level effectiveness remains constant from 6 October onwards. The piecewise control function  $C(t)$  and the ABCSMC procedure give a reasonable fit to data on new daily cases. The age distribution of confirmed cases is more skewed towards under 25s than the model predicts (Figure 4). Despite this discrepancy, the model underestimates the number of hospitalisations and hospital bed occupancy. This is possibly due to the concentration of the outbreak in high-risk populations, including Māori and Pasifika who are known to have a higher hospitalisation risk despite their structurally younger populations (19). The model overestimates the number of deaths to date, possibly due in part to a combination of the time lag from infection to death and stochasticity in small numbers. As increasing data from the current outbreak become available, it is reasonably



straightforward to update and apply alternative clinical pathway models to the simulation outputs for the number of new daily cases. This can be used to estimate admissions and occupancy of ward and ICU patients. The proportion of cases and the proportion of hospitalisations that are unvaccinated are slightly lower in the model than in reported data (Table 1). This could indicate that model assumptions on vaccine effectiveness are overly pessimistic. However, this discrepancy is likely affected by lower case ascertainment rates for vaccinated individuals with mild infection, and by the failure of the model to fully capture the observed skew towards younger age groups who have lower vaccination coverage.



**Figure 1.** Proportion of each age band who have had: (a) at least one dose; and (b) two doses. (c) Proportion of the eligible population (those aged over 12 years) who have had one dose or two doses. (d) The reproduction number at time  $t$  relative to the reproduction number in an unvaccinated population, calculated as  $\rho(NGM^v(t))/\rho(NGM)$ . Results are based on data on vaccinations administered up to 13 October 2021 and vaccine bookings for the period subsequent to 13 October 2021 in the Auckland metro region, with an additional assumption that everyone who has had one dose eventually receives their second dose. Results are plotted by the date each vaccine dose becomes effective in the model, which is assumed to be 14 days after it is administered.

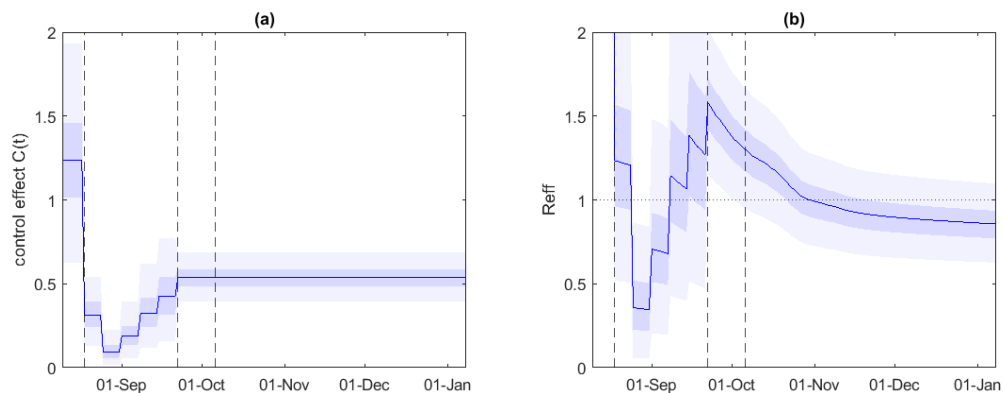


**Figure 2.** (a) Fitted control function  $C(t)$  and (b) time-varying reproduction number  $R_{eff}(t)$ , showing the median (solid curve), 50% CrI (dark blue shading) and 95% CrI (light blue shading) of the estimated posterior distribution. Dashed vertical lines show the start of alert level 4 (18 August), the move to Alert Level 3 in Auckland (22 September) and the move to alert level 3 “step 1” in Auckland (6 October).

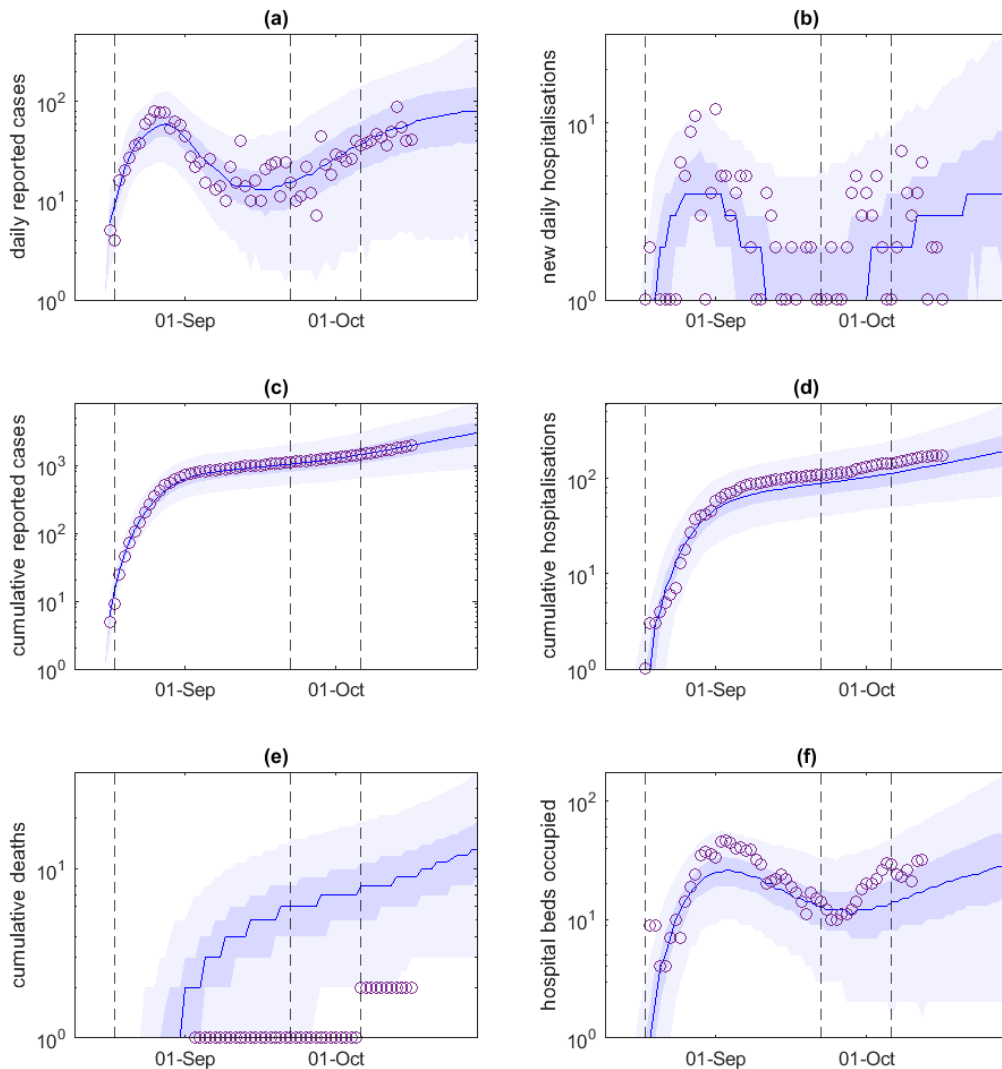


**Figure 3.** Outputs from model simulations showing: (a) daily reported cases; (b) daily hospital admissions; (c) cumulative reported cases; (d) cumulative hospital admissions; (e) cumulative deaths; (f) hospital beds occupied. Each graph shows the median (solid curve), 50% prediction interval (dark blue shading) and 95% prediction interval (light blue shading) for  $n = 1000$  simulations of the model, each with  $\theta$  chosen independently from the estimated posterior distribution. Note: reported daily case data and hospitalisation data covers the period from midnight to midnight each day and differs from the number of cases reported in the Ministry of Health's 1pm media releases.

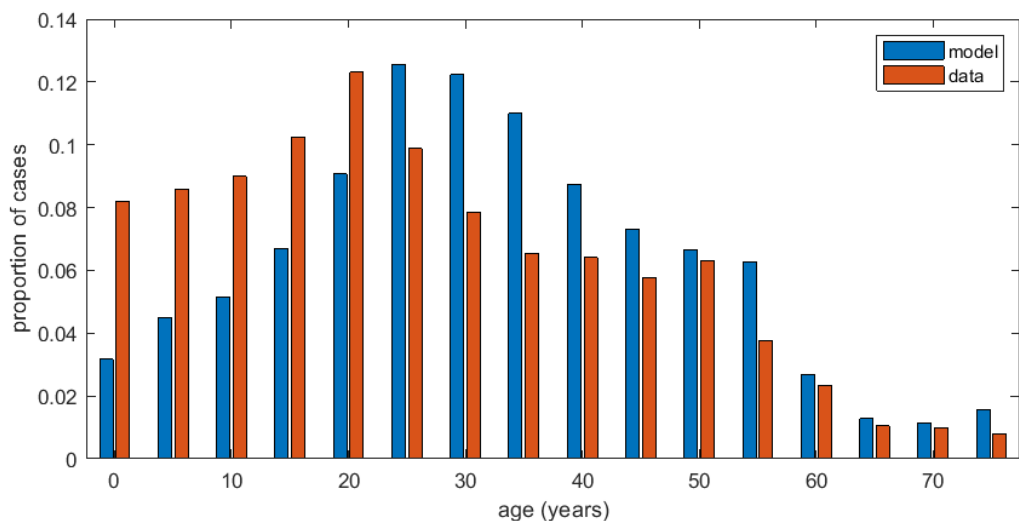


**Figure 4.** Age distribution of confirmed cases in 5-year age bands in the model outbreak up to 15 October 2021 (red) and in the model (blue).

	Cases		Hospitalisations	
	Model	Data	Model	Data
Unvaccinated	67.6%	84.0%	80.2%	90.5%
Partially vaccinated	19.0%	11.4%	12.7%	7.8%
Fully vaccinated	13.4%	4.5%	7.1%	1.7%

**Table 1.** Vaccination status of cases and hospitalisations between 17 August and 15 October 2021 in the model and as reported by the Ministry of Health (<https://www.health.govt.nz/our-work/diseases-and-conditions/covid-19-novel-coronavirus/covid-19-data-and-statistics/covid-19-case-demographics>). To be approximately consistent with model assumptions, unvaccinated includes those aged under 12 years and those who received their first dose less than 14 days prior to being reported as a case; partially vaccinated is those who had their first dose at least 14 days prior to being reported as a case and have either not had their second dose or had their second dose less than 14 days prior to being reported as a case; fully vaccinated is those who had both doses at least 14 days prior to being reported as a case.



## Future outbreak scenarios

Running realisations of the model with  $\theta$  sampled independently from the estimated posterior for a longer time period results in increasingly wide uncertainty intervals. In order to investigate different potential future trajectories and impacts of the outbreak following the easing of restrictions in Auckland on 6 October combined with ongoing vaccination, we ran 5 scenarios each with a fixed value of  $C(t)$  from 6 October onwards: 0.45, 0.50, 0.54, 0.58, 0.62 (Figures 5-9). The central scenario ( $C(t) = 0.54$ ) corresponds to the median posterior estimate and the five values approximately span the interquartile range of posterior estimates for  $C(t)$  for this time period. These scenarios correspond to values of  $R_{eff}(t)$  on 6 October of 1.1, 1.2, 1.3, 1.4, 1.5. However, note that ongoing vaccination results in a steady subsequent decline in the model value of  $R_{eff}(t)$  from its value on 6 October, as long as alert level restrictions continue.

The results show that in the low-transmission scenarios ( $C(t) = 0.45$  or  $0.50$ ), growth in cases is limited and increasing levels of immunity from vaccination bring the outbreak under control ( $R_{eff}(t) < 1$ ) within weeks (Figures 5-6). In the high-transmission scenarios ( $C(t) = 0.58$  or  $0.62$ ), cases grow much faster and it takes much longer for immunity to bring the outbreak under control if it happens at all (Figures 8-9). These scenarios result in a significant burden of hospitalisations. It is important to note that these scenarios do not take account of any increase in contact rates, for example as a result of any further easing of alert level restrictions subsequent to 6 October. Model outputs for the 25<sup>th</sup>, 50<sup>th</sup> and 75<sup>th</sup> percentile of the weekly number of infections, cases, hospital admissions, hospital beds occupied and deaths in each scenario are provided in the attached spreadsheets. Note these spreadsheets show numbers per week rather than per day.

The results in Figures 5-9 assume that the contact tracing system continues to provide the same level of reduction in transmission even at high case loads. This may not be possible in reality and this could cause an increase in  $R_{eff}$  (or at least a slowing in the rate at which immunity from vaccination brings  $R_{eff}$  down) and an acceleration of cases as contact tracing performance deteriorates. To explore the potential consequences of a deterioration in TTIQ performance, Figures 10-14 show the same five scenarios, but with an assumed contact tracing capacity of 1,000 active cases, defined as confirmed cases that are within 14 days of symptom onset. Note that 1,000 active cases corresponds to approximately 100 new confirmed cases per day on average. If the number of active cases exceeds the assumed capacity, contacts are no longer traced ( $p_{trace} = 0$ ), although we assume the probability of being tested remains at  $p_{test} = 0.45$ . The result of this is that the effectiveness of the TTIQ system drops from 20% to around 10% when capacity is exceeded, leading to a boost to  $R_{eff}$  of approximately 10%.

This is a highly simplified model of deterioration in TTIQ as cases grow. In reality, there will not be a single step change in one parameter but a gradual shift in multiple parameters including the number and type of contacts traced, the length of time taken to quarantine them, and possibly the effectiveness of quarantine and isolation as contacts and confirmed cases are less intensively managed and the capacity of managed isolation and quarantine (MIQ) facilities is limited. However, a more complex model would involve making more parameter assumptions with a paucity of data. If some contact tracing performance can be sustained, for example from quarantining household contacts and by automatic exposure notifications, the deterioration may be smaller than modelled. However, if the proportion of infections getting tested decreases, or the time taken to isolate cases lengthens, the deterioration in TTIQ performance could be worse. The results in Figures 10-14 should be



taken as indicative of a potential loss of contact tracing performance rather than a forecast of exactly when and to what extent this could occur.

Results for the low-transmission scenarios ( $C(t) = 0.45$  or  $0.50$ , Figures 10-11) are similar to those without any modelled contact tracing system capacity (Figures 5-6), because most model simulations remain under 1,000 active cases at these transmission rates. Results for the high-transmission scenarios ( $C(t) = 0.58$  or  $0.62$ , Figures 13-14) exhibit a transient flattening of new daily cases before accelerating again. This occurs because there is a reduction in the proportion of infections that are tested when contacts are no longer traced. Eventually the increase in  $R_{eff}$  translates into an increase in the case growth rate. These scenarios subsequently have many more cases, hospitalisations and deaths than the corresponding scenarios without any modelled contact tracing system capacity (Figures 8-9). These results suggest it is important to monitor contact tracing system performance metrics closely, even if daily new cases appear to flattening out. Signs of deterioration of contact tracing system performance could include an increase in the time taken to reach contacts, or a decrease in the proportion of contacts quarantined before symptom onset (21).

We also investigate the effect of a two-week circuit-breaker during which alert level 4 restrictions are applied, modelled as a reduction in the value of  $C(t)$  to 0.3 for a period of 14 days starting on 3 November (Figure 15). This value of  $C(t)$  is the model posterior estimate for the fourth week of alert level 4 restrictions (8–15 September), which is approximately double the estimate for the second and third weeks (25 August to 8 September). This models a lockdown that is reasonably effective in reducing contacts between people, but not as good as the peak estimated effectiveness of alert level 4 previously. We show results for the high-transmission scenario where  $C(t) = 0.62$  in the period from 6 October onwards (outside the two-week circuit-breaker period) and with the modelled contact tracing system capacity of 1,000 active cases.

The period of tighter restrictions reduces the number of new daily cases. With no circuit-breaker, the high-transmission scenario results in a total of around 2300 [960, 4200] hospitalisations and 160 [60, 310] deaths between 6 October 2021 and 8 January 2022. With the circuit-breaker, this is reduced to around 600 [220, 1200] hospitalisations and 40 [15, 90] deaths. These results are from a single scenario for current transmission rates and a single assumed contact tracing system capacity and should not be treated as forecasts. However, they do suggest that, in a scenario where cases are climbing steeply, the potential health benefits of a two-week period of tight restrictions are substantial. The likelihood of being able to eliminate the outbreak completely is negligible, but there are major benefits to delaying transmission while the vaccine rollout is still in progress. The end date of the model simulations (8 January 2022) is arbitrary and further hospitalisations and deaths would occur subsequent to this date in all scenarios. If the circuit-breaker merely postponed health impacts by two weeks it would not be justified. However, as approximately 7% of eligible Aucklanders are projected to become fully immunised during the two-week period from 3 November (Fig. 1), a circuit-breaker would allow time for significant additional population immunity to be built up via vaccination before community transmission increases further. Additional sensitivity analysis on the timing of the intervention shows that, if a two-week circuit-breaker is to be used, the earlier it is implemented the greater the benefits it provides. This is because earlier intervention maintains low levels of transmission for longer, which reduces the risk of overwhelming the contact tracing system and maximises the level of population immunity via vaccination before transmission rates rise.

None of the scenarios consider the effect of any easing of restrictions, for example reopening of schools, which would be expected to increase transmission further. This suggests that



increasing the number of people getting their first dose of the vaccine, over and above the number who already have a booking in the system, will be necessary to expediting a safe route out of lockdowns. Additional public health measures including mass masking, improved ventilation and air filtration, and widespread availability of rapid testing are also likely to be needed to dampen transmission and limit the pressure on the healthcare system.

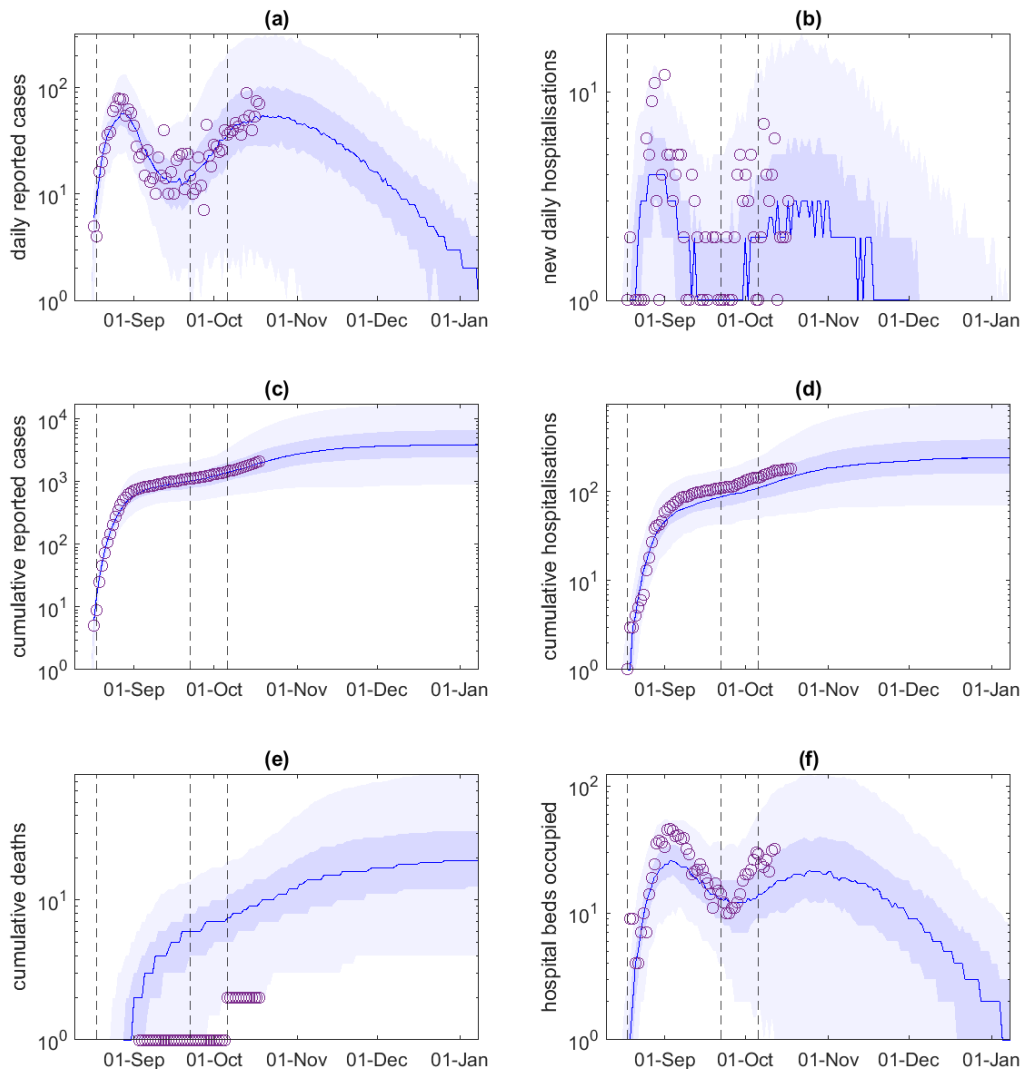


**Figure 5.** Model outputs for a very-low-transmission scenario where  $C(t) = 0.45$  from 6 October 2021 onwards: (a) daily reported cases; (b) daily hospital admissions; (c) cumulative reported cases; (d) cumulative hospital admissions; (e) cumulative deaths; (f) hospital beds occupied. Each graph shows the median (solid curve), 50% prediction interval (dark blue shading) and 95% prediction interval (light blue shading) for  $n = 200$  simulations of the model.

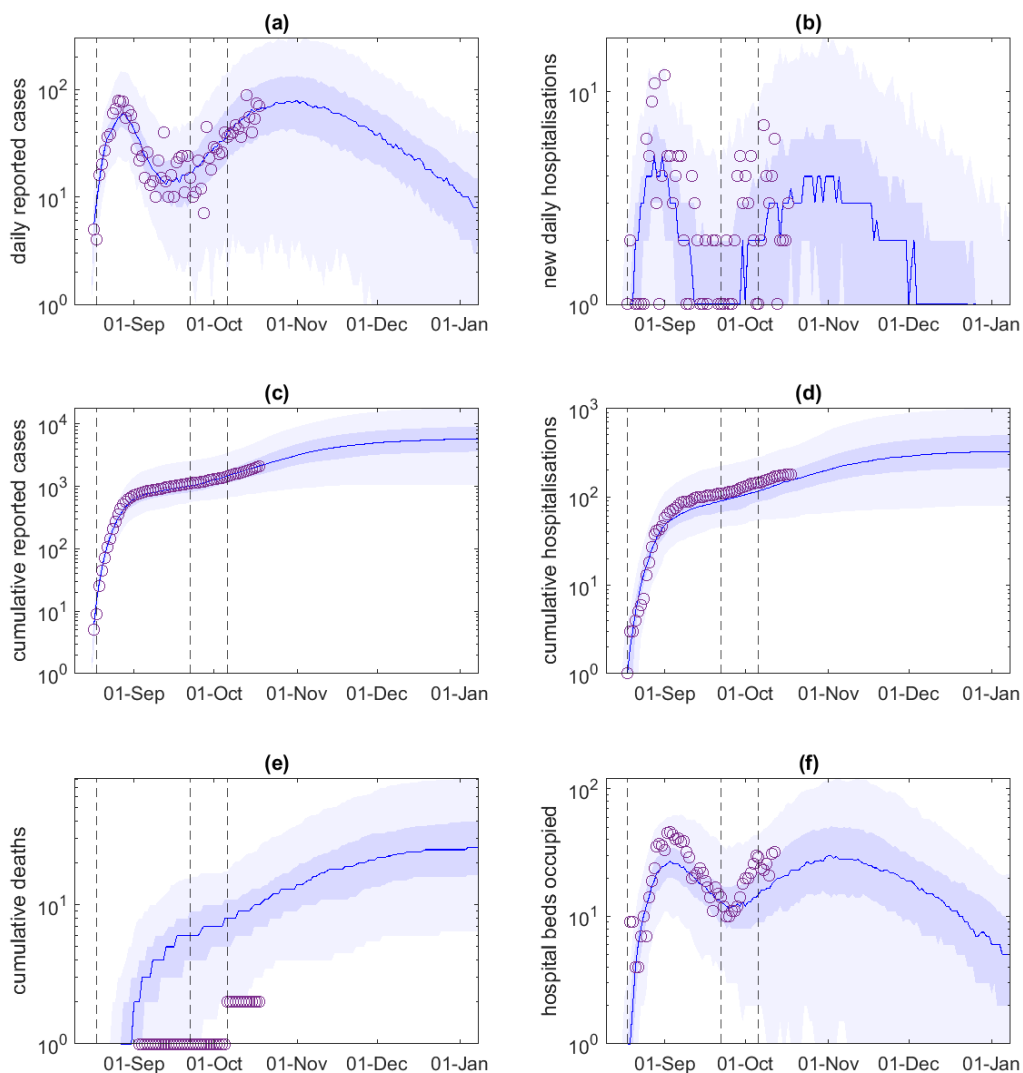


**Figure 6.** Model outputs for a low-transmission scenario where  $C(t) = 0.50$  from 6 October onwards: (a) daily reported cases; (b) daily hospital admissions; (c) cumulative reported cases; (d) cumulative hospital admissions; (e) cumulative deaths; (f) hospital beds occupied. Each graph shows the median (solid curve), 50% prediction interval (dark blue shading) and 95% prediction interval (light blue shading) for  $n = 200$  simulations of the model.

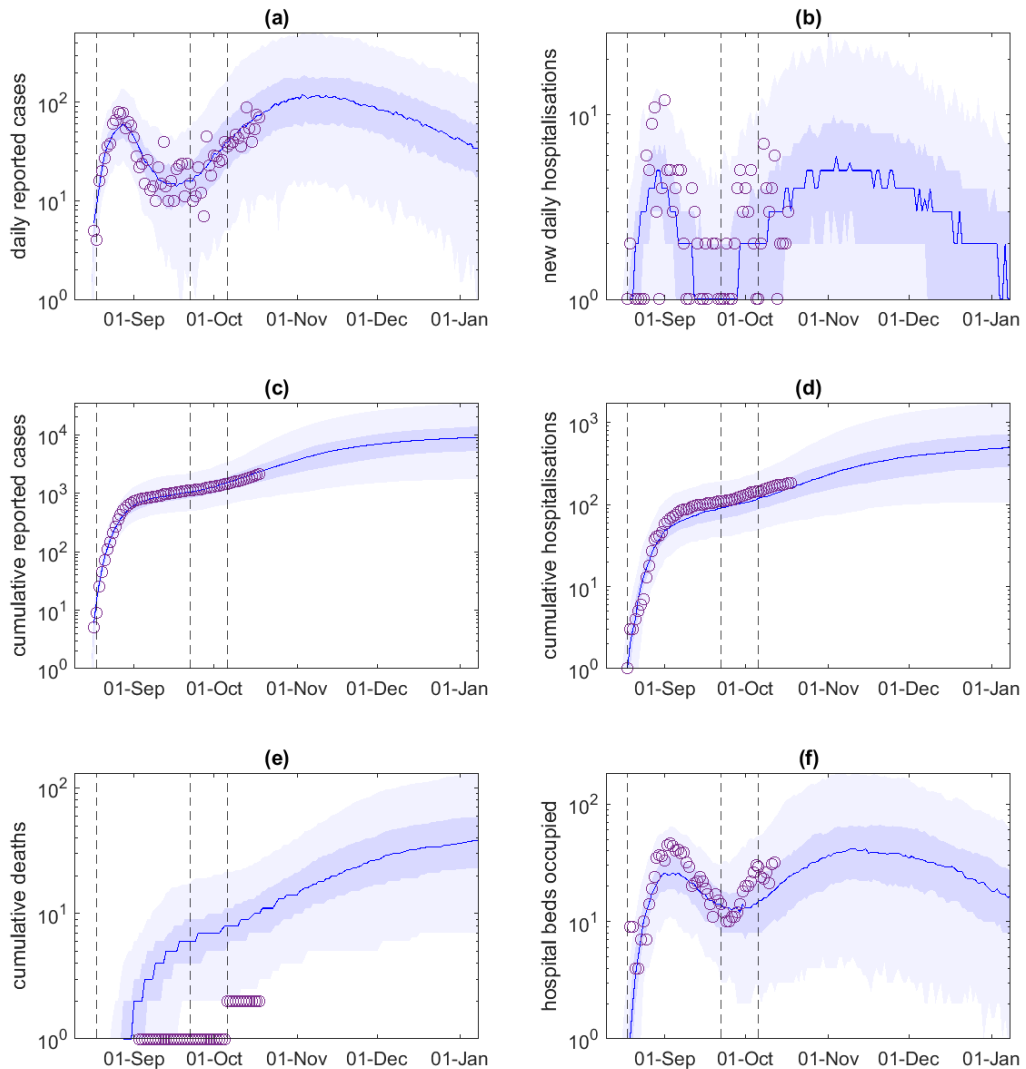


**Figure 7.** Model outputs for a medium-transmission scenario where  $C(t) = 0.54$  from 6 October onwards: (a) daily reported cases; (b) daily hospital admissions; (c) cumulative reported cases; (d) cumulative hospital admissions; (e) cumulative deaths; (f) hospital beds occupied. Each graph shows the median (solid curve), 50% prediction interval (dark blue shading) and 95% prediction interval (light blue shading) for  $n = 200$  simulations of the model.

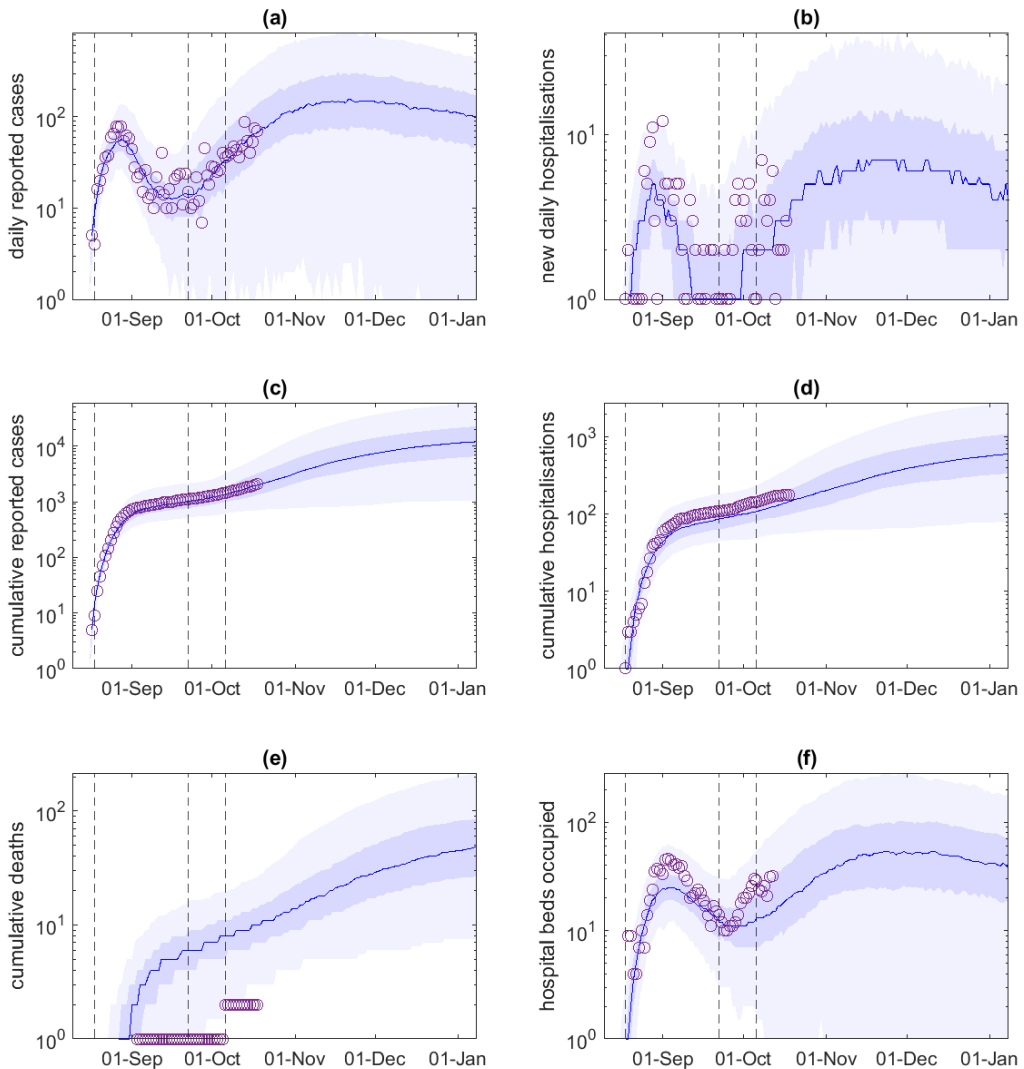


**Figure 8.** Model outputs for a high-transmission scenario where  $C(t) = 0.58$  from 6 October onwards: (a) daily reported cases; (b) daily hospital admissions; (c) cumulative reported cases; (d) cumulative hospital admissions; (e) cumulative deaths; (f) hospital beds occupied. Each graph shows the median (solid curve), 50% prediction interval (dark blue shading) and 95% prediction interval (light blue shading) for  $n = 200$  simulations of the model.

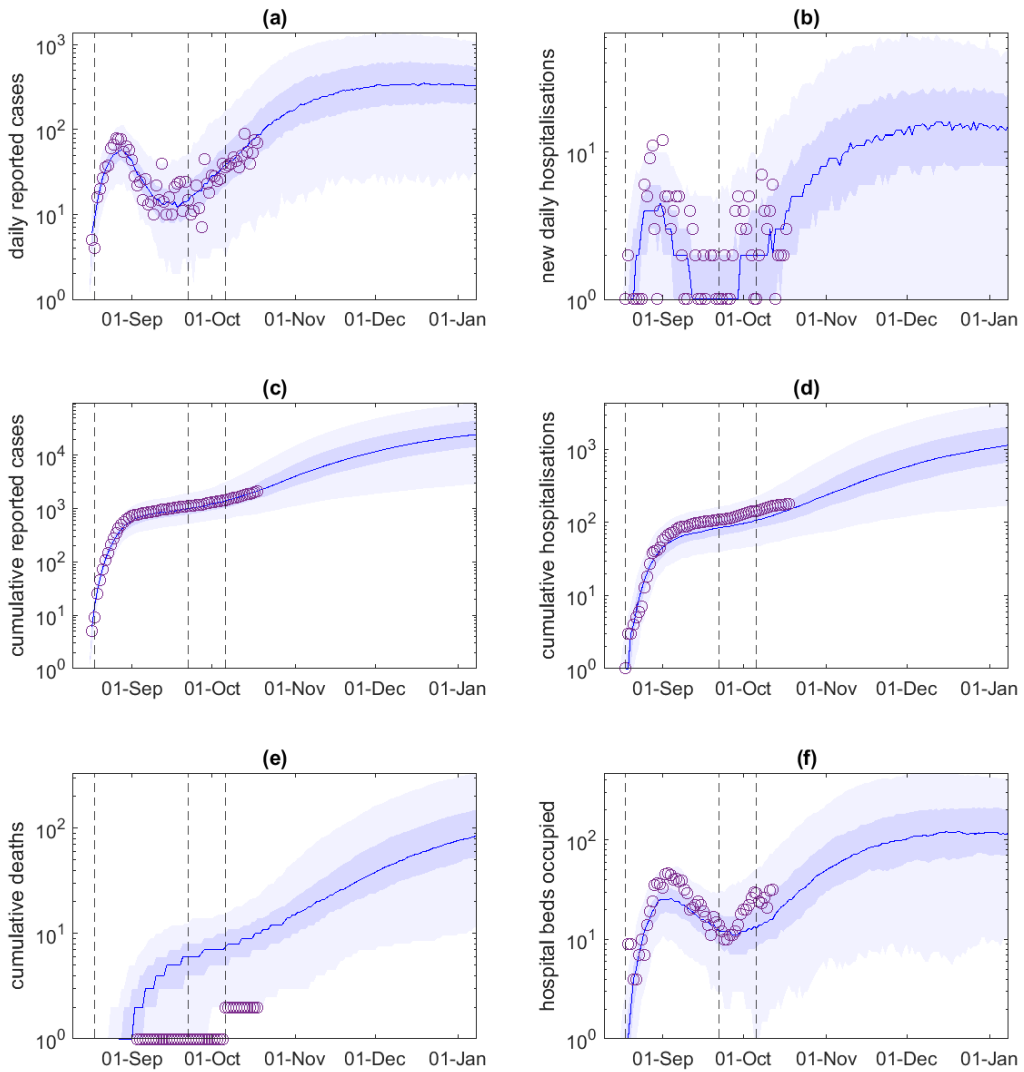


**Figure 9.** Model outputs for a very-high-transmission scenario where  $\mathcal{C}(t) = 0.62$  from 6 October onwards: (a) daily reported cases; (b) daily hospital admissions; (c) cumulative reported cases; (d) cumulative hospital admissions; (e) cumulative deaths; (f) hospital beds occupied. Each graph shows the median (solid curve), 50% prediction interval (dark blue shading) and 95% prediction interval (light blue shading) for  $n = 200$  simulations of the model.

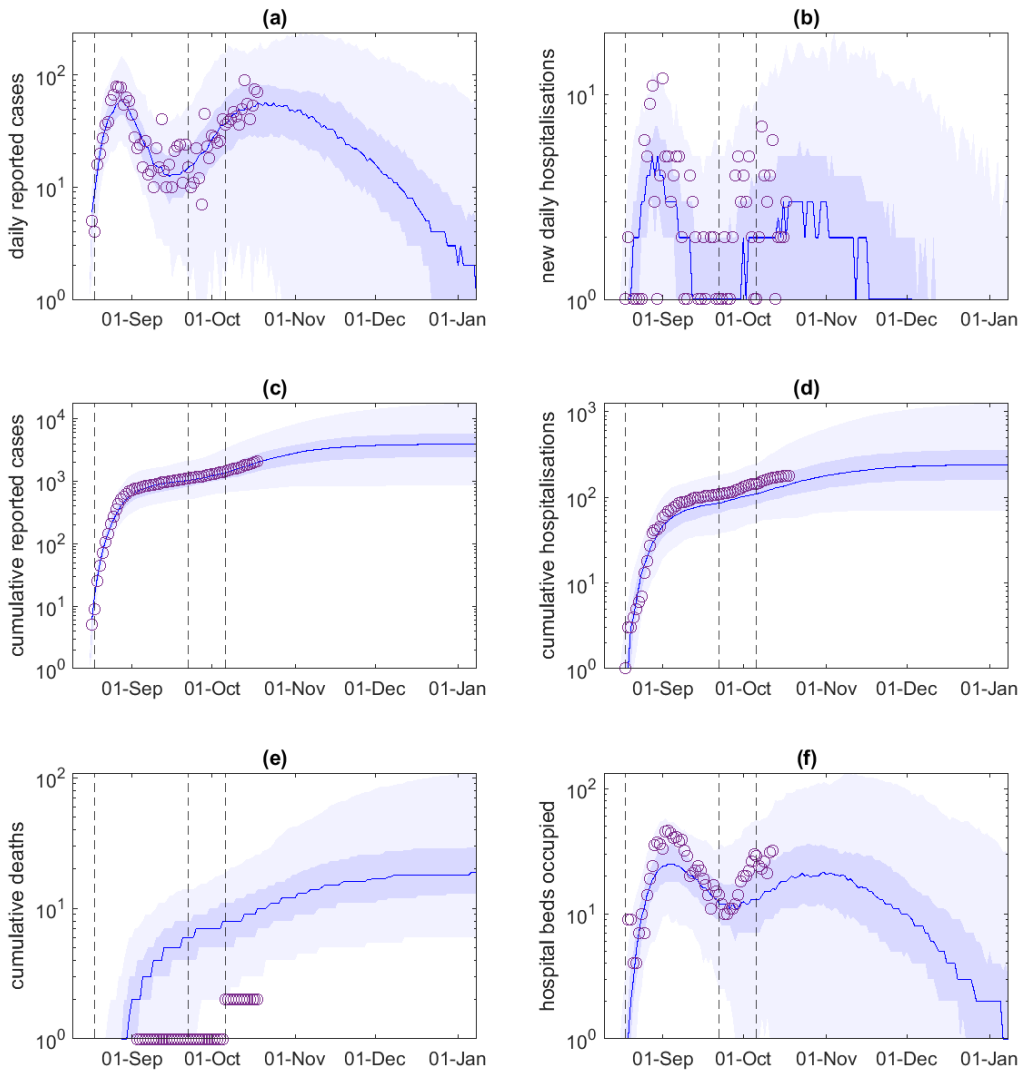


**Figure 10.** As for Figure 5 ( $C(t) = 0.45$  from 6 October onwards) but with a contact tracing system capacity of 1,000 active cases.

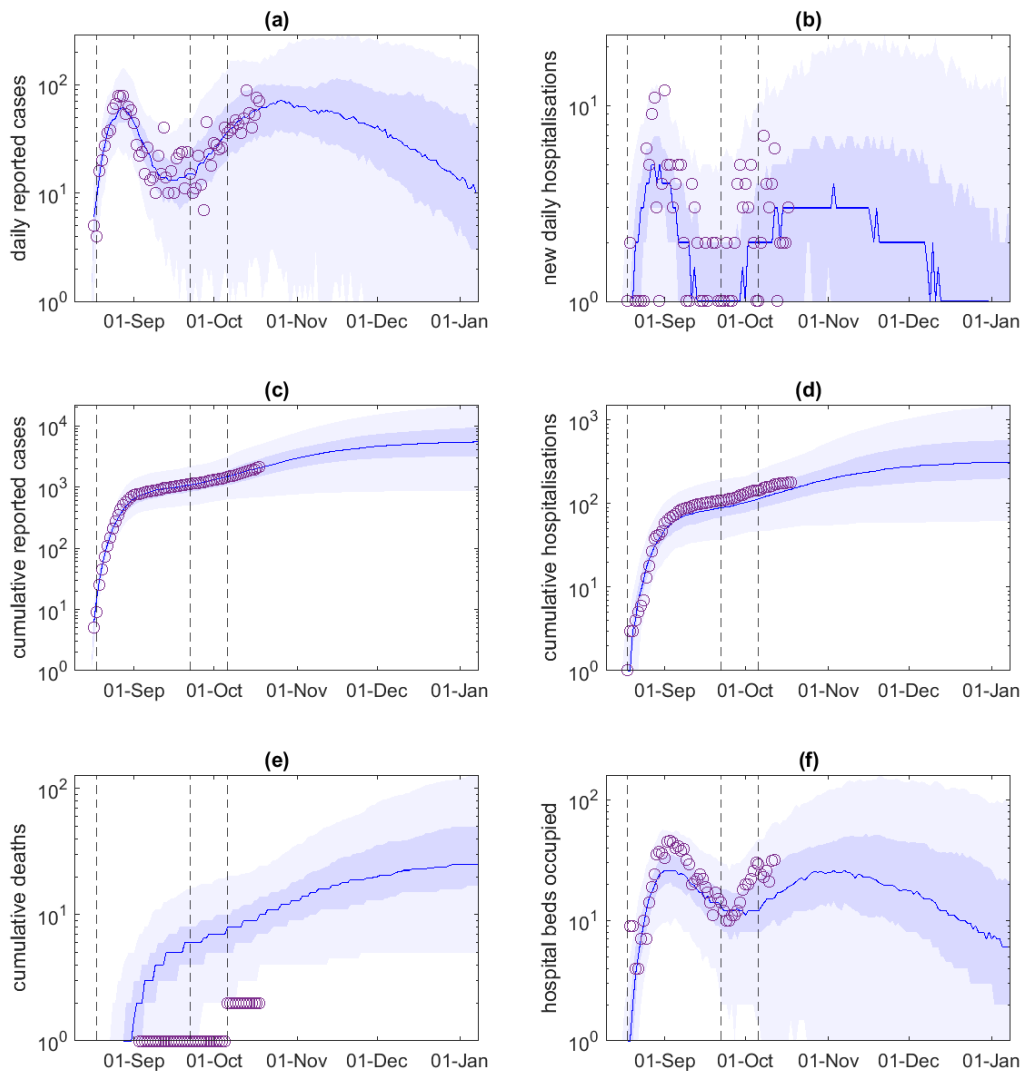


**Figure 11.** As for Figure 6 ( $C(t) = 0.50$  from 6 October onwards) but with a contact tracing system capacity of 1,000 active cases.

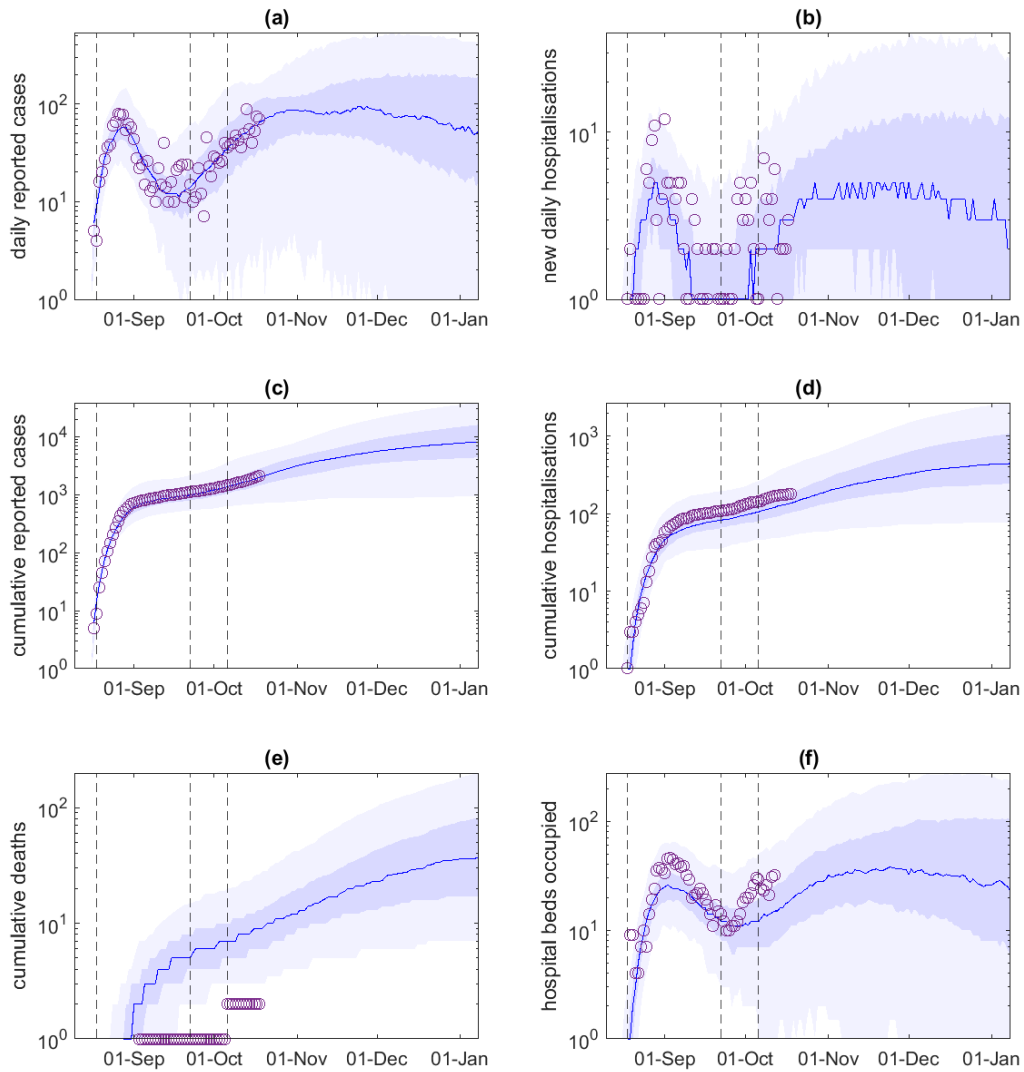


**Figure 12.** As for Figure 7 ( $C(t) = 0.54$  from 6 October onwards) but with a contact tracing system capacity of 1,000 active cases.

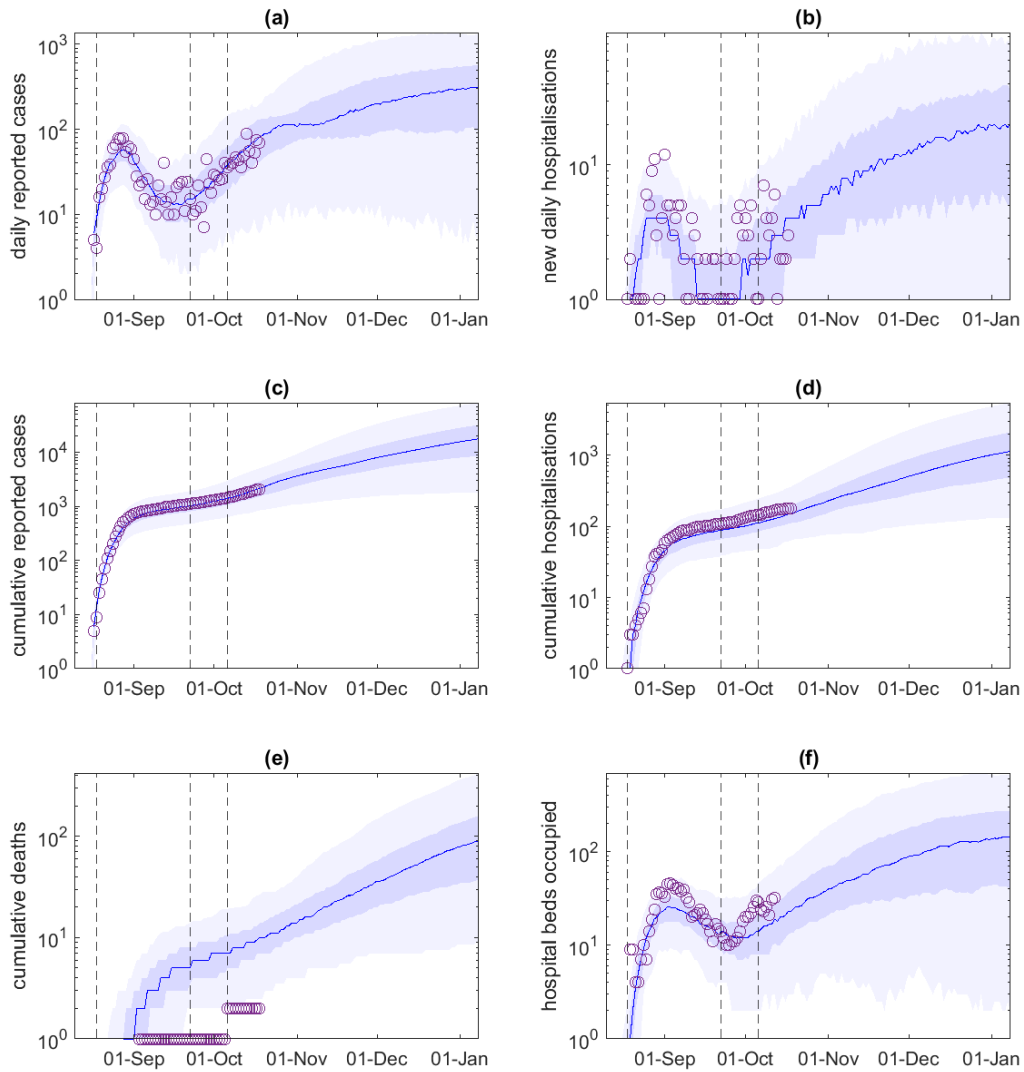


**Figure 13.** As for Figure 8 ( $C(t) = 0.58$  from 6 October onwards) but with a contact tracing system capacity of 1,000 active cases.

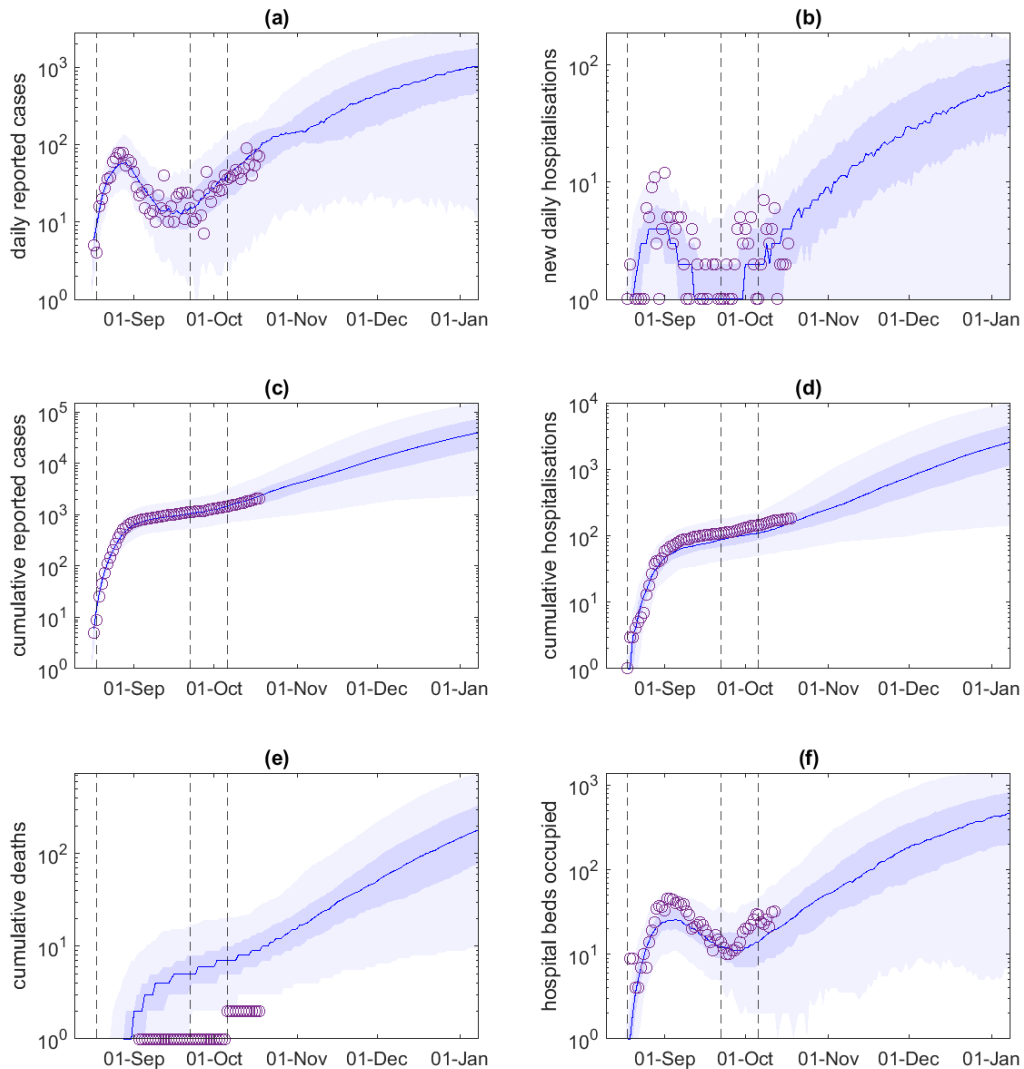


**Figure 14.** As for Figure 9 ( $C(t) = 0.62$  from 6 October onwards) but with a contact tracing system capacity of 1,000 active cases.

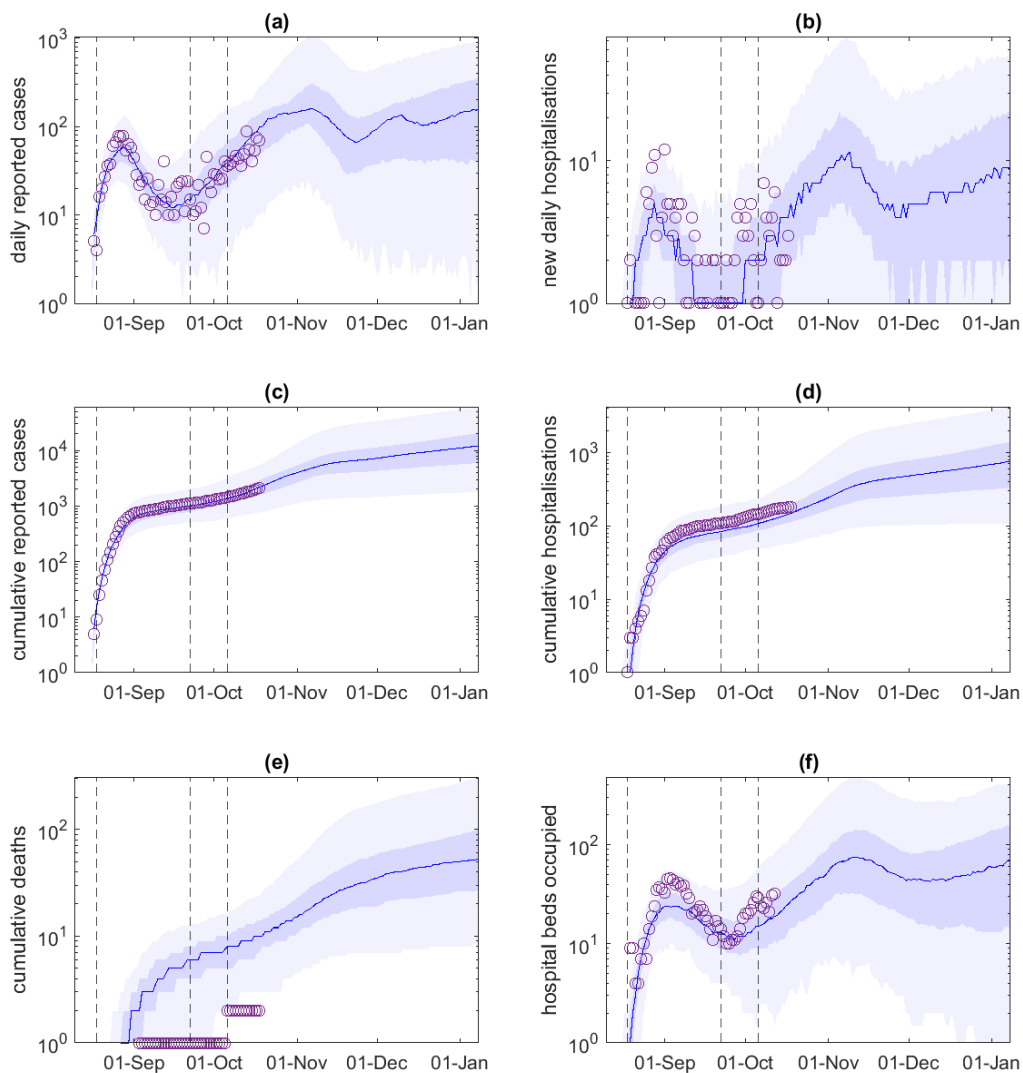


**Figure 15.** As for Figure 14 ( $C(t) = 0.62$  from 6 October onwards, contact tracing system capacity of 1,000 active cases) with a two-week circuit-breaker lockdown (modelled by  $C(t) = 0.3$ ) starting on 3 November 2021.

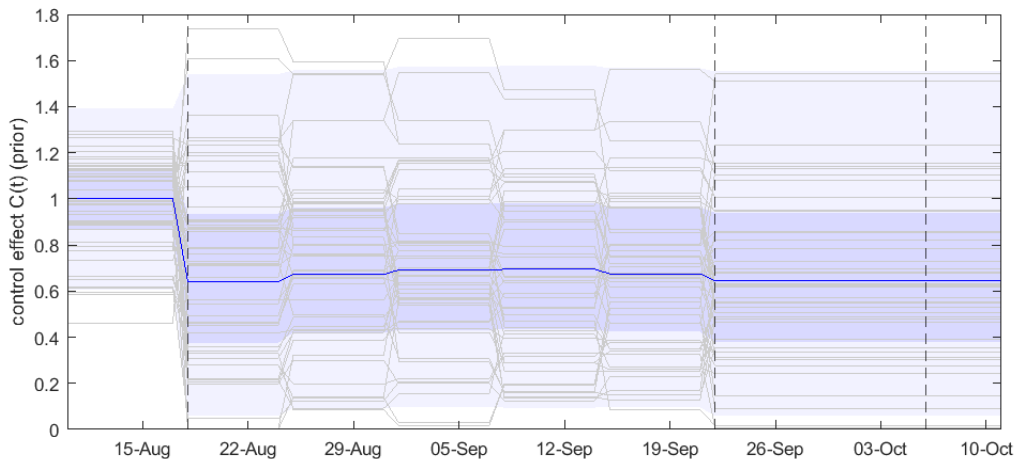


Parameter	Value
Basic reproduction number in the absence of control	$R_0 = 6$
Incubation period	Mean 5.5 days, s.d. 3.3 days
Generation interval	Mean 5.0 days, s.d. 1.9 days
Relative infectiousness of subclinical individuals	$\tau = 0.5$
Heterogeneity in individual reproduction number	$k = 0.5$
Vaccine effectiveness:	
- against infection (one dose)	$e_{I1} = 0.55$
- against infection (two doses)	$e_{I2} = 0.7$
- against transmission in breakthrough infection (one dose)	$e_{T1} = 0$
- against transmission in breakthrough infection (two doses)	$e_{T2} = 0.5$
- against severe disease in breakthrough infection (one dose)	$e_{D1} = 0.6$
- against severe disease in breakthrough infection (two doses)	$e_{D2} = 0.8$
Probability of a community case being tested	$p_{test} = 0.45$
Probability of a contact of a confirmed case being traced	$p_{trace} = 0.7$
Mean time from symptom onset to test result	4 days
Mean time from confirmation of case to quarantine of contacts	3 days
Length of hospital stay	Mean 8.0 days, s.d. 8.0 days

#### Age-specific parameters

Age (yrs)	0-4	5-9	10-14	15-19	20-24	25-29	30-34	35-39	40-44	45-49	50-54	55-59	60-64	65-69	70-74	75+
Pr(c clinical) (%)	54.4	55.5	57.7	59.9	62.0	64.0	65.9	67.7	69.5	71.2	72.7	74.2	75.5	76.8	78.0	80.1
Pr(h hosp)(%)	0.01	0.02	0.1	0.7	1.8	3.7	6.3	8.0	8.9	11.4	15.5	19.3	22.9	27.0	31.5	35.8
Pr(death)(%)	0.01	0.01	0.01	0.03	0.06	0.10	0.16	0.24	0.33	0.63	1.12	2.13	3.63	5.65	8.17	14.17
Susceptibility*	0.46	0.46	0.45	0.56	0.80	0.93	0.97	0.98	0.94	0.93	0.94	0.97	1.00	0.98	0.90	0.86
% of popn	6.2	6.6	6.5	6.3	7.3	8.5	8.3	7.5	6.5	6.6	6.3	6.0	5.0	4.0	3.3	5.1

**Table 1.** Parameter values used in the model. \*Susceptibility for age group  $i$  is stated relative to susceptibility for age 60-64 years. Age-dependent rates of clinical disease are based on (22). Age-dependent hospitalisation rates are based on (23) adjusted by a hazard ratio of 2.26 for the Delta variant (24). Infection fatality ratios are based on (23, 25) adjusted by an odds ratio of 2.32 for the Delta variant (26). Age-dependent susceptibility is based on (2).



**Supplementary Figure S1.** Prior for the control function  $C(t)$  showing the median (solid blue curve), 50% CrI (dark blue shading), 95% CrI (light blue shading), and 50 random draws from the prior (grey curves).

## Acknowledgements

The authors acknowledge the support of the New Zealand Ministry of Health, StatsNZ, and the Institute of Environment Science and Research in supplying data in support of this work. The authors are grateful to Samik Datta, Nigel French, Markus Luczak-Roesch, Melissa McLeod, Anja Mizdrak, Matt Parry, and the COVID-19 Modelling Government Steering Group for feedback on an earlier version of this report. This work was funded by the New Zealand Department of Prime Minister and Cabinet, Ministry of Business, Innovation and Employment COVID-19 Programme and Te Pūnaha Matatini, Centre of Research Excellence in Complex Systems.

## References

1. Steyn N, Plank MJ, Binny RN, Hendy S, Lustig A, Ridings K. A COVID-19 vaccination model for Aotearoa New Zealand. Pre-print. 2021.
2. Davies NG, Klepac P, Liu Y, Prem K, Jit M, group CC-w, et al. Age-dependent effects in the transmission and control of COVID-19 epidemics. *Nature Medicine*. 2020;26:1205-11.
3. Byambasuren O, Cardona M, Bell K, Clark J, McLaws M-L, Glasziou P. Estimating the extent of asymptomatic COVID-19 and its potential for community transmission: Systematic review and meta-analysis. *Official Journal of the Association of Medical Microbiology and Infectious Disease Canada*. 2020;5:223-34.
4. Buitrago-Garcia D, Egli-Gany D, Counotte MJ, Hossmann S, Imeri H, Ipekci AM, et al. Occurrence and transmission potential of asymptomatic and presymptomatic SARS-CoV-2 infections: A living systematic review and meta-analysis. *PLoS medicine*. 2020;17(9):e1003346.



5. Lauer SA, Grantz KH, Bi Q, Jones FK, Zheng Q, Meredith HR, et al. The incubation period of coronavirus disease 2019 (COVID-19) from publicly reported confirmed cases: estimation and application. *Annals of internal medicine*. 2020;172(9):577-82.
6. Ferretti L, Wymant C, Kendall M, Zhao L, Nurtay A, Abeler-Dörner L, et al. Quantifying SARS-CoV-2 transmission suggests epidemic control with digital contact tracing. *Science*. 2020;368(6491).
7. Ryu S, Kim D, Lim J-S, Ali ST, Cowling BJ. Changes in the serial interval and transmission dynamics associated with the SARS-CoV-2 Delta variant in South Korea. *medRxiv*. 2021.
8. Pung R, Mak TM, Kucharski AJ, Lee VJ. Serial intervals in SARS-CoV-2 B. 1.617. 2 variant cases. *The Lancet*. 2021;398(10303):837-8.
9. Kang M, Xin H, Yuan J, Ali ST, Liang Z, Zhang J, et al. Transmission dynamics and epidemiological characteristics of Delta variant infections in China. *medRxiv*. 2021.
10. Zhang M, Xiao J, Deng A, Zhang Y, Zhuang Y, Hu T, et al. Transmission dynamics of an outbreak of the COVID-19 Delta variant B. 1.617. 2—Guangdong Province, China, May–June 2021. *China CDC Weekly*. 2021;3(27):584-6.
11. Li B, Deng A, Li K, Hu Y, Li Z, Xiong Q, et al. Viral infection and transmission in a large well-traced outbreak caused by the Delta SARS-CoV-2 variant. *medRxiv*. 2021.
12. Public Health England. Vaccine effectiveness expert panel - consensus narrative. 2021.
13. SPI-M-O. Summary of further modelling of easing restrictions – Roadmap Step 4 on 19 July 2021. 2021.
14. Prem K, Cook AR, Jit M. Projecting social contact matrices in 152 countries using contact surveys and demographic data. *PLoS computational biology*. 2017;13(9):e1005697.
15. James A, Plank MJ, Hendy S, Binny RN, Lustig A, Steyn N. Model-free estimation of COVID-19 transmission dynamics from a complete outbreak. *PLoS ONE*. 2020;16:e0238800.
16. Riou J, Althaus CL. Pattern of early human-to-human transmission of Wuhan 2019 novel coronavirus (2019-nCoV), December 2019 to January 2020. *Eurosurveillance*. 2020;25(4):2000058.
17. Lloyd-Smith JO, Schreiber SJ, Kopp PE, Getz WM. Superspreading and the effect of individual variation on disease emergence. *Nature*. 2005;438(7066):355-9.
18. Moore S, Hill EM, Tildesley MJ, Dyson L, Keeling MJ. Vaccination and non-pharmaceutical interventions for COVID-19: a mathematical modelling study. *The Lancet Infectious Diseases*. 2021;21(6):793-802.
19. Steyn N, Binny RN, Hannah K, Hendy S, James A, Lustig A, et al. Māori and Pacific People in New Zealand have higher risk of hospitalisation for COVID-19. *New Zealand Medical Journal*. 2021;134(1538):28-43.
20. Toni T, Welch D, Strelkowa N, Ipsen A, Stumpf MP. Approximate Bayesian computation scheme for parameter inference and model selection in dynamical systems. *Journal of the Royal Society Interface*. 2009;6(31):187-202.



21. James A, Plank MJ, Binny RN, Lustig A, Steyn N, Hendy S, et al. Successful contact tracing systems for COVID-19 rely on effective quarantine and isolation. medRxiv. 2020.
22. Hinch R, Probert W, Nuray A, Kendall M, Wymant C, Hall M, et al. Effective configurations of a digital contact tracing app: A report to NHSX. 2020;16 April 2020:29.
23. Verity R, Okell LC, Dorigatti I, Winskill P, Whittaker C, Imai N, et al. Estimates of the severity of coronavirus disease 2019: a model-based analysis. *The Lancet Infectious Diseases*. 2020.
24. Twohig KA, Nyberg T, Zaidi A, Thelwall S, Sinnathamby MA, Aliabadi S, et al. Hospital admission and emergency care attendance risk for SARS-CoV-2 delta (B. 1.617. 2) compared with alpha (B. 1.1. 7) variants of concern: a cohort study. *The Lancet Infectious Diseases*. 2021.
25. Levin AT, Hanage WP, Owusu-Boaitey N, Cochran KB, Walsh SP, Meyerowitz-Katz G. Assessing the age specificity of infection fatality rates for COVID-19: systematic review, meta-analysis, and public policy implications. *European journal of epidemiology*. 2020;1-16.
26. Fisman DN, Tuite AR. Evaluation of the relative virulence of novel SARS-CoV-2 variants: a retrospective cohort study in Ontario, Canada. *CMAJ*. 2021.